

Critical Coagulation Concentration of a Salt-Free Colloidal Dispersion

Jyh-Ping Hsu and Hsiu-Yu Yu

Department of Chemical Engineering, National Taiwan University, Taipei, Taiwan 10617

Shiojenn Tseng*

Department of Mathematics, Tamkang University, Tamsui, Taipei, Taiwan 25137

Received: January 5, 2006; In Final Form: February 20, 2006

Both exact and approximate analytical solutions of the Poisson–Boltzmann equation for two planar, parallel surfaces are derived for the case when a dispersion medium contains counterions only, and the results obtained are used to evaluate the critical coagulation concentration of a spherical dispersion. A correction factor, which is a function of the valence of counterions, the surface potential of a particle, and the potential on the midplane between two particles at the onset of coagulation, is derived to modify the classic Schulze–Hardy rule for the dependence of the critical coagulation concentration on the valence of counterions. The correction factor is found to increase with the increase in the valence of counterions and/or with the increase in the surface potential. However, it approaches a constant value of 0.8390 if the surface potential is sufficiently high.

1. Introduction

Salt-free dispersion, where its dispersion medium contains no or a negligible amount of ionic species except for those dissociated from the dispersed entities, is one of the important dispersed systems in practice. A dispersion of polyelectrolyte, for instance, belongs to this category where the dissociation of the functional groups on polyelectrolyte molecules yields a charged backbone and the dissociated counterions are released to the surrounding liquid phase. Natural polyelectrolytes are ubiquitous in living tissues. Typical examples include DNA^{1,2} and RNA, the carriers of gene code, and filamentous actin (F-actin) and microtubules.² While aqueous environments which contain structural molecules are called gels, cornea and striated muscle are termed biological polyelectrolyte gels.^{3,4} Synthetic polyelectrolytes are widely used in both daily commodities such as the water-absorbing materials in diapers and laboratory- and industrial-scaled processes such as reverse osmosis, ion-exchange, and oil recovery.⁵ Compared with relevant analyses for typical colloidal dispersions, those for salt-free dispersions are very limited. Afrey et al.⁶ solved analytically the Poisson–Boltzmann equation describing the electrical potential for the case of a cylindrical particle. Adopting the theories of Imai and Oosawa⁷ and Oosawa,⁸ Ohshima⁹ derived an analytical surface charge density–surface potential expression for a spherical particle. The corresponding expression for the case when a dispersion medium contains only a small amount of added salts was also derived.¹⁰

The critical coagulation concentration, defined as the minimum concentration of counterions required to induce coagulation, is one of the most important basic properties of a colloidal dispersion and is often applied to assess its status. Historically, the critical concentration is described by the Schulze–Hardy rule, an empirical relation based on experimental observations which states that the critical coagulation concentration of counterions is proportional to the inverse sixth-power of its valence. This rule was interpreted theoretically by DLVO

(Derjaguin, Landau, Verwey, and Overbeek) theory.¹¹ While later investigations revealed that the Schulze–Hardy rule is not general enough to cover the behaviors of counterions commonly encountered in practice, it is still widely referred to due to its concise nature. One of the basic steps in DLVO theory is to evaluate the electrical interaction energy between two spherical particles. This involves solving a Poisson–Boltzmann equation describing the spatial variation of electrical potential. Up to now, the only analytically solvable problem for an arbitrary level of electrical potential is that for an isolated planar surface remaining at constant surface potential in a symmetric electrolyte solution. For other cases, either an approximate analytical approach^{12–19} or a numerical procedure is necessary.

In this study the critical coagulation concentration of a spherical, salt-free colloidal dispersion is derived on the basis of the solution of the Poisson–Boltzmann equation for two parallel planar surfaces. A correction factor, which is a function of the valence of counterions, the surface potential of a particle, and the potential on the midplane between two particles at the onset of coagulation, is derived to modify the classic Schulze–Hardy rule.

2. Analysis

Let us consider a monodispersed, positively charged spherical particle of radius a_0 in a salt-free medium containing only counterions of valence b . At the onset of coagulation, since the separation distance between two particles is small, the local curvature of a particle is insignificant; that is, it can be assumed to be planar. Referring to Figure 1, d is the distance between two particles, ψ_s is the surface potential, and ψ_m is the potential on the midplane between two particles, which is also the minimum potential of the present system. If we let $\psi(r)$ be the potential at a distance r from the left particle, then it can be described by the Poisson–Boltzmann equation

$$\frac{d^2\psi(r)}{dr^2} = \frac{bFC_b^0}{\epsilon} \exp\left[\frac{bF\psi(r)}{RT}\right] \quad (1)$$

* To whom correspondence should be addressed. Tel: 886-2-26215656 ext 2508. Fax: 886-2-26209916. E-mail: topology@mail.ktu.edu.tw.

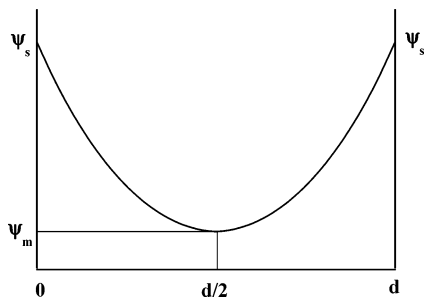


Figure 1. Spatial distribution of ψ for the case of two identical planar surfaces where d is the separation distance between surfaces, ψ_s is the surface potential, and ψ_m is the potential at $r = d/2$.

where C_b^0 and ϵ are, respectively, the molar concentration of anions and the permittivity of the dispersion medium, and F , R , and T are, respectively, the Faraday constant, the gas constant, and the absolute temperature. Equation 1 can be rewritten in dimensionless form as

$$\frac{d^2 y}{dx^2} = \frac{1}{b} e^{by} \quad (2)$$

where $y = F\psi/RT$ and $x = \kappa r$, $\kappa = (2IF^2/\epsilon RT)^{1/2}$ being the Debye–Hückel parameter and $I = C_b^0 b^2/2$ the ionic strength.

The symmetric nature of the present problem suggests that only the domain $0 \leq x \leq D/2$ needs to be considered, where $D = \kappa d$ is the scaled separation distance between two particles. The corresponding boundary conditions are

$$y = y_s, x = 0 \quad (3)$$

$$y = y_m, x = \frac{D}{2} \quad (4)$$

where $y_s = F\psi_s/RT$ and $y_m = F\psi_m/RT$. The solution to eq 2 subject to these boundary conditions is

$$y = \frac{1}{b} \ln \left\{ e^{by_m} \sec^2 \left\{ -\sqrt{\frac{e^{by_m}}{2}} x + \tan^{-1} [e^{b(y_s - y_m)} - 1]^{1/2} \right\} \right\}, \quad 0 \leq x \leq \frac{D}{2} \quad (5)$$

Applying eq 4, this expression implies that y_m must satisfy

$$-\sqrt{\frac{e^{by_m}}{2}} \frac{D}{2} + \tan^{-1} [e^{b(y_s - y_m)} - 1]^{1/2} = 0 \quad (6)$$

This equation has to be solved numerically for y_m . However, if $\exp[b(y_s - y_m)] \gg 1$, since $\tan^{-1}[\exp[b(y_s - y_m)] - 1]^{1/2}$ can be approximated by $(\pi/2) - \exp[b(y_m - y_s)/2]$, eq 5 yields

$$y_m = \frac{-2}{b} \ln \left(\frac{D}{\sqrt{2\pi^2}} + \frac{2}{\pi} e^{-by_s/2} \right) \quad (7)$$

For convenience, we define two specific boundary conditions by letting $y_m = y_m$ and $y_m \rightarrow 0$ in this expression and solving the resultant expressions to give

$$D = \sqrt{2\pi} e^{-by_m/2} - 2\sqrt{2} e^{-by_s/2}, y_m = y_m \quad (8)$$

and

$$D_{\text{inf}} \rightarrow \sqrt{2\pi} - 2\sqrt{2} e^{-by_s/2}, y_m \rightarrow 0 \quad (9)$$

Here, D_{inf} can be viewed as the separation distance between two particles at which the interaction between the corresponding two double layers is negligible. Based on eqs 8 and 9 and the change of variables through $dD = -(b\pi/\sqrt{2})e^{-(1/2)by_m} dy_m$, it can be shown that the osmotic pressure p and the electrical energy between two planar surfaces V_p are

$$\frac{p}{IRT} = \frac{2}{b^2} (e^{by_m} - 1) \quad (10)$$

$$\frac{\kappa V_p}{IRT} = -\frac{1}{\kappa} \int_{\infty}^D \frac{p}{IRT} dD = \frac{2\sqrt{2}\pi}{b^2} (e^{by_m/2} + e^{-by_m/2} - 2) \quad (11)$$

At the onset of coagulation, Derjaguin approximation¹¹ is applicable to the estimation of the electrical energy between two spherical particles. Applying this approximation, it can be shown that the electrical energy between two spherical particles is

$$V_e = \frac{\pi a}{\kappa^2} \int_D^{\infty} V_p dD \quad (12)$$

where $a = \kappa a_0$ is the scaled radius of a particle. Substituting eq 11 into this expression yields

$$\frac{\kappa^3 V_e}{\pi a IRT} = \frac{2\pi^2}{b^2} [-3 + y_m b - e^{-by_m} + 4e^{-by_m/2}] \quad (13)$$

According to DLVO theory, the total energy $V_t(D)$ is the sum of the electrical repulsive energy $V_e(D)$ and the van der Waals attractive energy $V_a(D)$, that is, $V_t(D) = V_e(D) + V_a(D)$. For the present case

$$V_a = -\frac{Aa}{12D} \quad (14)$$

where A is the Hamaker constant. At the critical coagulation concentration, $C_b^0 = C_{b,c}^0$, and the following conditions need to be satisfied²⁰

$$V_t = 0 \text{ and } \frac{dV_t}{dD} = 0 \quad (15)$$

where D_c is the scaled separation distance between two particles at the onset of coagulation. According to eq 8

$$y_m = y_{m,c}, D_c = \sqrt{2\pi} e^{-by_{m,c}/2} - 2\sqrt{2} e^{-by_s/2} \quad (16)$$

where $y_{m,c}$ denotes the value of y_m at the onset of coagulation. Substituting eqs 13 and 14 into eq 15, we obtain

$$C_{b,c}^0 = \frac{144\pi^6 R^5 T^5 \epsilon^3}{A^2 F^6 b^6} (-3 + by_{m,c} - e^{-by_{m,c}} + 4e^{-by_{m,c}/2})^2 (\sqrt{2\pi} e^{-by_{m,c}/2} - 2\sqrt{2} e^{-by_s/2})^2 \quad (17)$$

3. Results and Discussion

Substituting eq 7 into eq 5 yields an approximate analytical solution of eq 2

$$y = \frac{1}{b} \ln \left\{ \left(\frac{D}{\sqrt{2}\pi} + \frac{2}{\pi} e^{-by_s/2} \right)^{-2} \sec^2 \left\{ - \left(\frac{D}{\pi} + \frac{2\sqrt{2}}{\pi} e^{-by_s/2} \right)^{-1} x + \tan^{-1} \left[e^{by_s} - \left(\frac{D}{\sqrt{2}\pi} + \frac{2}{\pi} e^{-by_s/2} \right)^{-2} - 1 \right]^{1/2} \right\} \right\}, 0 \leq x \leq \frac{D}{2} \quad (18)$$

which is applicable for the case when $\exp[b(y_s - y_m)] \gg 1$. Figure 2 shows the spatial distribution of the scaled potential between two planes (y/y_s) calculated by the approximate analytical expression, eq 5, at various levels of y_s for the case when $b = 3$. For comparison, the corresponding exact values of (y/y_s) obtained by solving eq 2 numerically are also presented. Figure 2 reveals that if $\exp[b(y_s - y_m)] \gg 1$, the performance of eq 5 is satisfactory. Note that the higher the level of y_s the faster is the rate of decrease in (y/y_s). This is because the double layer is compressed at a high surface potential, the so-called counterion condensation,^{8,21} which leads to a fast decay in the potential as the distance from a surface increases.

Typical variations of the scaled osmotic pressure (p/IRT) and the scaled electrical energy ($\kappa V_p/IRT$) between two planar surfaces, and the variation of the scaled electrical energy between two spherical particles based on Derjaguin approximation ($\kappa^3 V_e/\pi a IRT$) as a function of the scaled separation distance D are shown in Figure 3. As expected, all these quantities decline with the increase in the surface potential and with the increase in D .

In the evaluation of the critical coagulation concentration of counterions, $C_{b,c}^0$, the scaled electrical potential on the mid-plane between two particles at the onset of coagulation, $y_{m,c}$, plays an important role. The variations of $y_{m,c}$ at various values of y_s and b are summarized in Figure 4. Note that if the repulsive electrical energy between two particles is large, coagulation between them does not occur. Also, since we assume that $\exp[b(y_s - y_m)] \gg 1$ in the derivation of eq 7, the data which lead to a difference between $\tan^{-1}[\exp(b(y_s - y_m)) - 1]^{1/2}$ and $(\pi/2) - \exp[(b(y_m - y_s)/2)]$ exceeds $|15\%|$ are excluded in Figure 4. According to eqs 7, 10, and 13, y_m , p , and V_e all increase with the increase in y_s . This implies that as y_s increases the coagulation between two particles is retarded unless the separation distance between them is small enough so that the short-ranged van der Waals force dominates. Figure 4 shows that $y_{m,c}$, and consequently V_e , declines with the increase in b , which arises

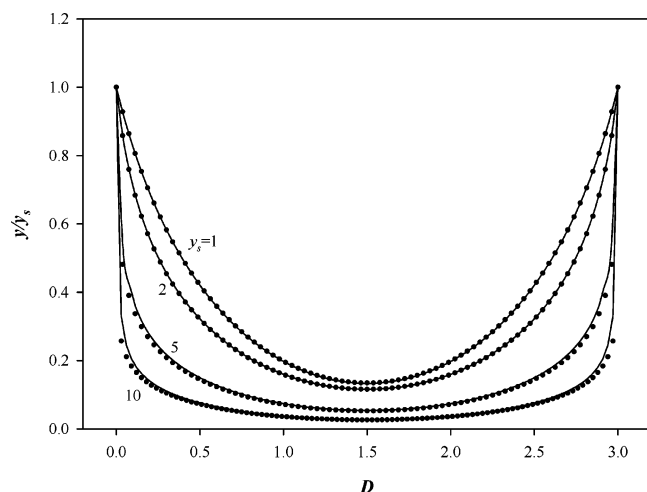


Figure 2. Spatial distribution of scaled electrical potential (y/y_s) between two planes at various levels of y_s for the case when $b = 3$: solid curves, results based on eq 5; discrete symbols, exact results by solving eq 2 numerically.

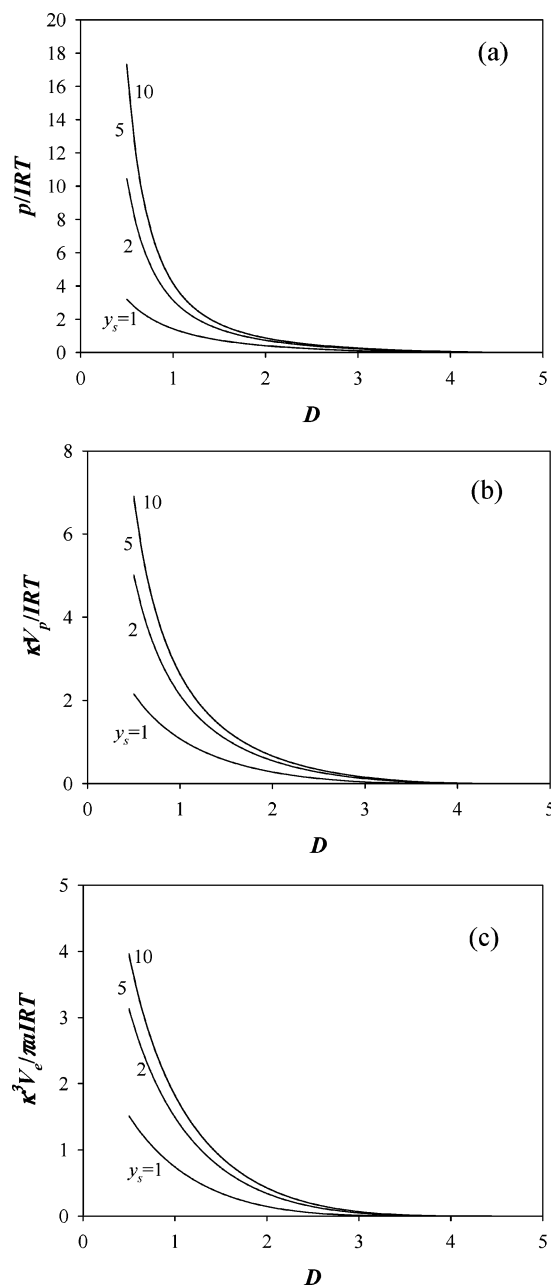


Figure 3. Variation of (a) scaled osmotic pressure between two identical planes p/IRT , (b) scaled electrical energy between two identical planes ($\kappa V_p/IRT$), and (c) scaled electrical energy between two identical spheres ($\kappa^3 V_e/\pi a IRT$), as a function of scaled separation distance $D = \kappa d$, where κ is based on $b = 3$, at various values of y_s .

from the decrease in the thickness of double layer. Also, for a fixed value of b , $y_{m,c}$ increases with the increase in y_s , and approaches a constant when y_s is sufficiently high.

The simulated scaled separation distance between two particles at the onset of coagulation, D_c , the value of D at which the interaction between two double layers is negligible, D_{inf} , and the ratio (D_c/D_{inf}) are presented in Figures 5 through 7. As in the case of Figure 4 the criterion $\exp[b(y_s - y_m)] \gg 1$ needs to be satisfied. Figures 5 and 6 indicate that both D_c and D_{inf} decline as the valence of counterions increases, which is expected. For a fixed value of b , D_c decreases with the increase in y_s , and the reverse is true for D_{inf} . The former is because that if the surface potential is high, so is the stability of a dispersion, and, therefore, the separation distance between two particles at the onset of coagulation becomes short. The latter is because

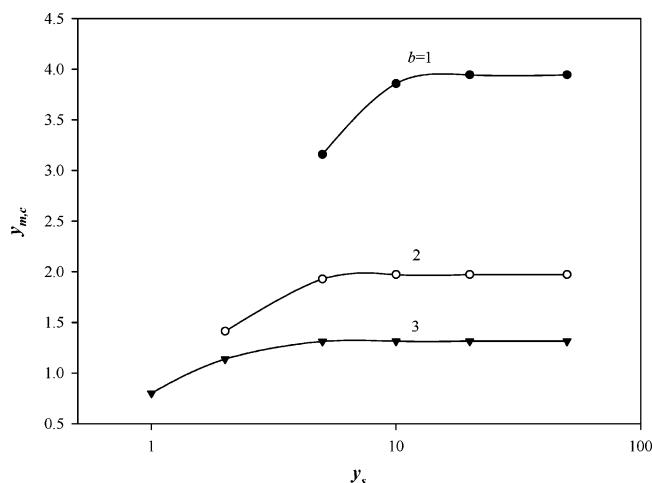


Figure 4. Variation of $y_{m,c}$ as a function of y_s at various values of b .

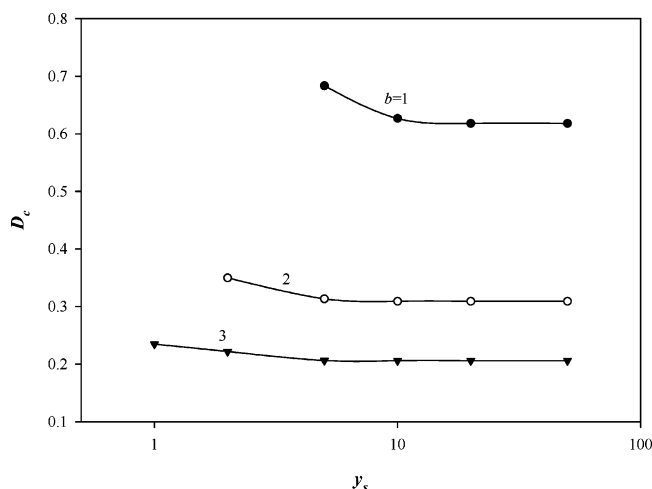


Figure 5. Variation of D_c as a function of y_s at various values of b with κ based on $b = 1$.

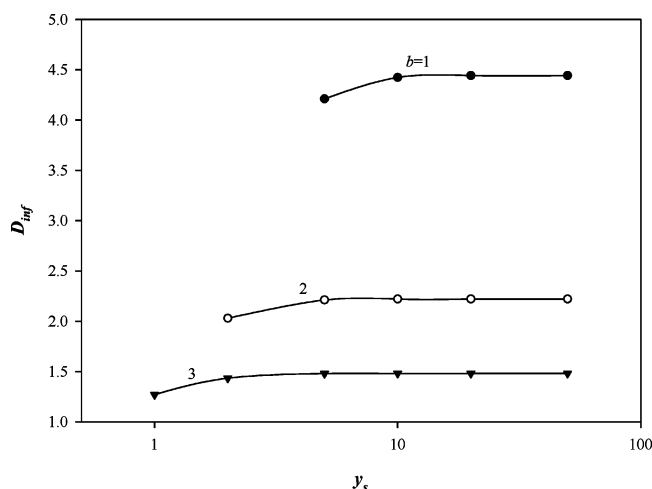


Figure 6. Variation of D_{inf} as a function of y_s at various values of b with κ based on $b = 1$.

the higher the surface potential the longer is the distance needed for the electrical potential to decay to a low value. Figures 5 and 6 show that if y_s is sufficiently high, both D_c and D_{inf} approach a constant. According to Figure 7, for a fixed value of b , (D_c/D_{inf}) decreases rapidly with the increase in y_s , which implies that the higher the surface potential the more important its influence on the stability of a dispersion is. However, if y_s

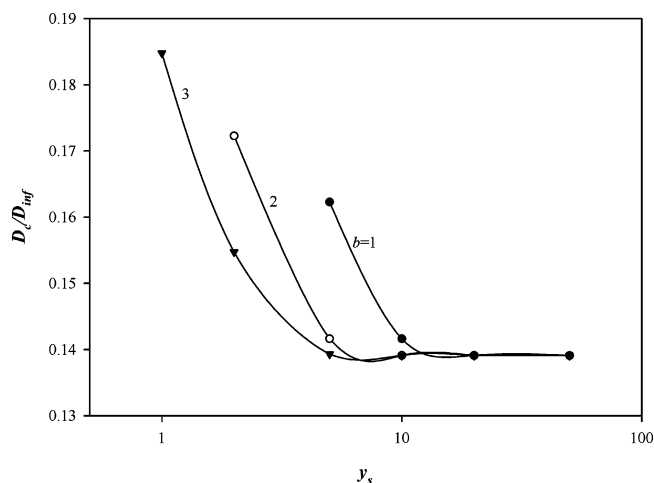


Figure 7. Variation of (D_c/D_{inf}) as a function of y_s at various values of b with κ based on $b = 1$.

TABLE 1: Variation of the Ratio $(C_{b,c}^0/C_{3,c}^0)$ at Various Combinations of y_s and b^a

b	y_s						Schulze–Hardy rule
	1	2	5	10	20	50	
1			361.027	685.692	728.697	729.000	729.000
2		5.624	10.768	11.386	11.391	11.391	11.391
3	1.000	1.000	1.000	1.000	1.000	1.000	1.000

^a The last column shows the results predicted by the Schulze–Hardy rule.

exceeds about 10, $(D_c/D_{inf}) = 0.1391$, regardless of the value of b , and its influence becomes unimportant.

Table 1 summarizes the values of $(C_{b,c}^0/C_{3,c}^0)$ at various combinations of y_s and b , where $C_{3,c}^0$ is the value of $C_{b,c}^0$ at $b = 3$. This table reveals that as the surface potential increases $(C_{b,c}^0/C_{3,c}^0)$ approaches to that predicted by Schulze–Hardy rule, that is, the ratio of the critical coagulation concentrations for counterions of valences 3, 2, and 1 is $3^{-6}:2^{-6}:1^{-6}$, or roughly 1:11:729. This is consistent with the result of DLVO theory, which is based on the assumption of a high surface potential. According to eq 17

$$C_{b,c}^0 = Kb^{-6}F_{a,c} \quad (19)$$

where

$$K = \frac{144\pi^6 R^5 T^5 \epsilon^3}{A^2 F^6} \quad (20)$$

is a constant and

$$F_{a,c} = (-3 + by_{m,c} - e^{-by_{m,c}} + 4e^{-by_{m,c}/2})(\sqrt{2\pi}e^{-by_{m,c}/2} - 2\sqrt{2}e^{-by_s/2})^2 \quad (21)$$

a factor which is influenced by b , y_s , and $y_{m,c}$. This factor can be viewed as a measure for the degree of deviation of the Schulze–Hardy rule from a more accurate result. Figure 8 shows the variation of $F_{a,c}$ as a function of y_s at various valence of counterions, b . This figure reveals that for a fixed surface potential, if its level is not high, $F_{a,c}$ increases with the increase in the value of b , and for a fixed value of b , it increases with the increase in the surface potential. Note that regardless of the value of b , $F_{a,c}$ approaches a constant value of 0.8390 if y_s exceeds about 10.

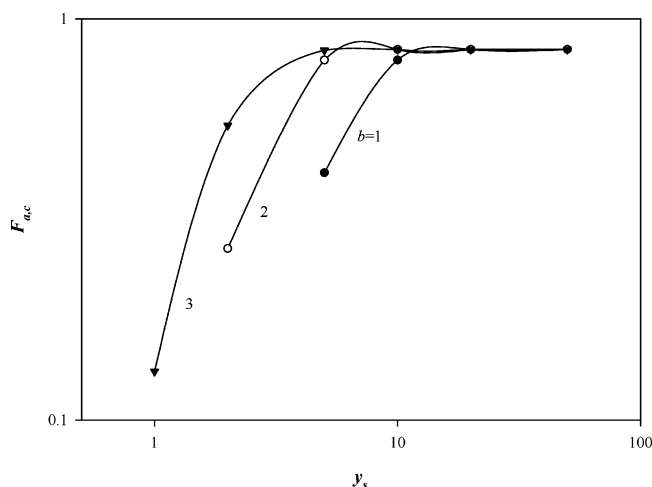


Figure 8. Variation of F_{ac} as a function of scaled surface potential y_s at various values of b .

4. Conclusions

Both exact and approximate analytical expressions for the electrical potential and the electrical energy between two identical, planar parallel particles are derived for the case when the dispersion medium contains counterions only, and the results are used to evaluate the critical coagulation concentration of a spherical dispersion. We show that the classic Schulze–Hardy rule for the dependence of the critical coagulation concentration on the valence of counterions is applicable to the present system subject to a correction factor, which is a function of the valence of counterions, the surface potential of a particle, and the potential on the mid-plane between two particles at the onset of coagulation. The results of numerical simulation reveal that

the correction factor increases with the increase in the valence of counterions and/or with the increase in the surface potential of a particle. However, it approaches a constant value of 0.8390, which is independent of the valence of counterions, if the surface potential of a particle is sufficiently high.

Acknowledgment. This work is supported by the National Science Council of the Republic of China.

References and Notes

- (1) Korolev, N.; Lyubartsev, A. P.; Nordenskiöld, L. *Biophys. J.* **1998**, *75*, 3041.
- (2) Pfohl, T.; Li, Y.; Kim, J. H.; Wen, Z.; Wong, G. C. L.; Koltover, I.; Kim, M. W.; Safinya, C. R. *Colloids Surf. A* **2002**, *198–202*, 613.
- (3) Elliott, G. F.; Hodson, S. A. *Rep. Prog. Phys.* **1998**, *61*, 1325.
- (4) Regini, J. W.; Elliott, G. F. *Int. J. Biol. Macromol.* **2001**, *28*, 245.
- (5) Nagvekar, M.; Tihminlioglu, F.; Danner, R. P. *Fluid Phase Equilibria* **1998**, *145*, 15.
- (6) Afrey, T.; Berg, P. W.; Morawetz, H. *J. Polym. Sci.* **1951**, *7*, 543.
- (7) Imai, N.; Oosawa, F. *Busseiron Kenkyu* **1952**, *52*, 42.
- (8) Oosawa, F. *Polyelectrolytes*; Dekker: New York, 1971.
- (9) Ohshima, H. *J. Colloid Interface Sci.* **2002**, *247*, 18.
- (10) Ohshima, H. *J. Colloid Polym. Sci.* **2004**, *282*, 1185.
- (11) Hunter, R. J. *Foundations of Colloid Science*; Oxford University Press: New York, 1992; Vol. 1.
- (12) Hsu, J. P.; Kuo, Y. C. *J. Colloid Interface Sci.* **1994**, *167*, 35.
- (13) Hsu, J. P.; Kuo, Y. C. *J. Colloid Interface Sci.* **1997**, *185*, 530.
- (14) Wang, Z. W.; Yi, X. Z.; Li, G. Z.; Guan, D. R.; Lou, A. J. *Chem. Phys.* **2001**, *274*, 57.
- (15) Wang, Z. W.; Li, G. Z.; Guan, D. R.; Lou, A. J. *J. Colloid Interface Sci.* **2002**, *246*, 302.
- (16) Tuinier, R. *J. Colloid Interface Sci.* **2003**, *258*, 45.
- (17) Tseng, S.; Jiang, J. M.; Hsu, J. P. *J. Colloid Interface Sci.* **2004**, *273*, 218.
- (18) Hsu, J. P.; Lin, S. H.; Tseng, S. *J. Phys. Chem. B* **2004**, *108*, 4495.
- (19) Lin, S. H.; Hsu, J. P.; Tseng, S.; Chen, C. J. *J. Colloid Interface Sci.* **2005**, *281*, 255.
- (20) Verwey, E. J. W.; Overbeek, J. Th. G. *Theory of the Stability of Lyophobic Colloids*; Elsevier: Amsterdam, 1948.
- (21) Manning, G. S. *J. Chem. Phys.* **1969**, *51*, 924.